Nitrogen doping into titanium dioxide by the sol-gel method using nitric acid

Hiromasa Nishikiori,* Yosuke Fukasawa, Yuta Yokosuka, Tsuneo Fujii

Department of Environmental Science and Technology, Graduate School of Science and Technology, Shinshu University, 4-17-1 Wakasato, Nagano 380-8553, Japan

* Corresponding author

E-mail: nishiki@shinshu-u.ac.jp

Phone: +81-26-269-5536

FAX: +81-26-269-5550

Abstract

N-doped TiO_2 has been prepared by use of sol-gel systems containing titanium alkoxide, with nitric acid as the nitrogen source. The time needed for gelation of the systems was drastically reduced by ultrasonic irradiation. The peaks assigned to the nitrate and nitrous ions were observed by FT-IR measurement during the sol-gel reaction. The N-doping was confirmed by observation of N-O peaks in the XPS spectrum of the sample heated at 400 °C. The nitrate ion acted as an oxidizer of the ethanol solvent and titanium species. The TiO_2 became doped with nitrogen oxide species were doped as a result of reduction of nitrate ion incorporated into the dried gel samples. These results indicated that the added nitric acid was reduced during the sol-gel transition and heating process, and the resulting NO species were situated in the titania networks. The UV and visible photocatalytic activity of the samples was confirmed by the degradation of trichloroethylene.

Keywords: titanium dioxide; nitrogen doping; nitric acid; ultrasonic irradiation; photocatalyst

Introduction

TiO_2 acts as a photocatalyst only when irradiated with UV light of wavelength shorter than approximately 400 nm, because it has a band gap energy of about 3.0 eV [1,2]. To enable use of solar and household light for the degradation of pollutants or harmful compounds, the development of visible-light-driven photocatalysts has attracted much attention [2]. It is important to prepare the visible-light-driven photocatalyst by a simple method. Many scientists have investigated the preparation, structure, and activity of N-doped TiO_2 because its mechanism of action is simple and it is readily available [2]. The N-doped TiO_2 photocatalysts are generally prepared by treating TiO_2 with NH_3, for example, heating TiO_2 in an NH_3 gas atmosphere [3–7]. Recently, N-doped TiO_2 has also been prepared by chemical vapor deposition [8,9], liquid phase deposition [10], and plasma techniques, for example plasma-based ion implantation [11] or plasma-assisted molecular beam epitaxy [12]. Visible-light sensitive TiO_2 photocatalysts have also been prepared by wet-method N-doping, i.e., calcination of the hydrolysis products of titanium tetraisopropoxide or titanium salts with an aqueous NH_3 solution [13–15]. One of the wet methods, the sol-gel method, is also used to obtain uniform TiO_2 nano-sized crystalline particles. Not only TiO_2 but also N-doped TiO_2 can be prepared by the sol-gel method. The N-doped TiO_2 can be prepared from sol-gel precursor solution containing various

nitrogen compounds, for example urea or alkyl amines [16–19].

These preparation procedures for N-doped TiO_2 are based on oxidation of the reduced nitrogen species, for example NH_3, by the titanium species. We have prepared N-doped TiO_2 by the sol-gel method using a large amount of nitric acid as the source of nitrogen [20] as Dong et al. previously reported [21]. A large amount of nitric acid was required because most of it was evaporated during the heating process. Nitric acid, which is often used as an acid catalyst in the sol-gel process to prepare TiO_2 [22,23], is the most oxidized form of nitrogen. It is expected that nitric acid is reduced during the process of preparation of TiO_2 and doped into the titania networks because it also acts as an oxidizer. However, this method requires a low temperature, approximately room temperature, and a long time, approximately 30 days, to prepare the titania gel, because a rapid sol-gel reaction causes evaporation of the nitric acid and rapid disassembly of the system.

In this study, we tried to shorten the time needed for gelation of the sol-gel system containing titanium alkoxide and nitric acid at low temperature by ultrasonic irradiation. Ultrasonic irradiation accelerates the sol-gel reaction because the violent agitation promotes the collision of the titanium alkoxide molecules and evaporation of the solvent. Changes in the nitrogen species were observed by FT-IR measurement during the sol-gel reaction in order to clarify the nitrogen-doping mechanism. The N-doping was confirmed by XPS analysis

of the heated samples. The UV and visible photocatalytic activity of this sample was examined by the degradation of trichloroethylene.

Experimental

Materials

Titanium tetraisopropoxide (TTIP), nitric acid (69–70%), hydrochloric acid (35%), trichloroethylene (TCE), and ethanol of S reagent-grade were obtained from Wako Pure Chemicals, and the dry nitrogen gas and dry air (ca. nitrogen 79% + oxygen 21%) were obtained from Okaya Sanso and used without further purification. The water was deionized and distilled by use of a distiller (Yamato WG23).

Preparation of photocatalysts

The sol-gel system used to prepare the normal TiO_2 consisted of 6.8 cm^3 TTIP, 40 cm^3 ethanol, and 1.0 cm^3 hydrochloric acid as a catalyst for the sol-gel reaction. The sol-gel systems used to prepare the N-doped TiO_2 consisted of 6.8 cm^3 TTIP, 40 cm^3 ethanol, and 0.21, 1.0, 5.0, or 10.0 cm^3 nitric acid as the catalyst and a source of nitrogen. TTIP was added dropwise to the mixture of the other materials in a glove box filled with dry nitrogen gas at ambient temperature. The systems were stirred during the addition, and then for an additional 15 min. The reaction occurred during ultrasonic irradiation. Gelation of all

the systems was observed 6 days after starting the ultrasonic irradiation although it took 30 days without any ultrasonic irradiation. The resulting dry gels were heated at 400°C for 3 h. The photocatalyst samples prepared from sols containing 0, 0.21, 1.0, 5.0, and 10.0 cm^3 nitric acid were labeled N0, N02, N1, N5, and N10, respectively.

Characterization of photocatalysts

The prepared photocatalyst samples were characterized by SEM (Hitachi S-4000), XRD analysis using CuKα radiation (Rigaku RINT2000), and XPS using AlKα radiation (ULVAC PHI 5600). The size of the crystallites of each sample was estimated from the full-width at half-maximum of the 25.3° peak in the XRD pattern by use of Sherrer's equation, $D = 0.9\lambda/\beta \cdot \cos\theta$. The specific surface areas of the samples were measured by the volumetric gas adsorption method using nitrogen gas (BEL Japan; BELSORP-mini). The spectroscopic properties of the samples were analyzed by UV-visible diffuse reflectance spectroscopy (Shimadzu UV3150) and FTIR spectroscopy (Shimadzu FTIR-8300). The FTIR measurement was conducted during the sol-gel reaction with and without ultrasonic irradiation in order to observe the changes in the nitrogen species. For FTIR measurements, the sol samples were placed between two KBr single crystal plates whereas the gel and crystalline powder samples were pressed into KBr pellets.

The amounts of TCE and dichloroacetyl chloride (DCAC; a product of the TCE

degradation) adsorbed on the samples were estimated by gas chromatography-mass spectrometry (Shimadzu GCMS-QP5000). Each photocatalyst sample (10 mg) was placed in a glass vial. Gaseous TCE and DCAC diluted with dry air were injected into the vials at concentrations of 3.2×10^{-4} and 1.3×10^{-4} mol dm^{-3}, respectively. The adsorption ability of the samples for TCE and DCAC was estimated from the concentrations determined by GC-MS analysis after equilibration of their adsorption.

Photocatalytic degradation of TCE

Each photocatalyst sample (250 mg) was placed in an infrared cell made of Pyrex glass. Two plates of KBr single crystals were used as the infrared windows and were sealed by Teflon O-rings. The TCE gas diluted with dry air was injected into the infrared cell in which its concentration was 3.2×10^{-4} mol dm^{-3}. The cell was kept at ambient temperature until the adsorption of TCE had equilibrated. The degradation reaction of the TCE was carried out in the cell by near-UV light irradiation from a 4-W black light bulb (Toshiba FL4BLB) and visible light from a 150 W xenon lamp (Hamamatsu Photonics C2577) with a 420-nm cutoff filter. The FTIR spectra (Shimadzu FTIR-8300) of the gas phase in the cell were obtained as a function of light irradiation time. Changes in the concentrations of TCE and the products were determined during TCE degradation with the prepared photocatalyst samples. We can assume that the chemical species that existed in the reaction cell are in

equilibrium between the gas phase and the catalyst surface. Therefore, the decomposed species on the catalyst surface appear in the FTIR spectra.

Results and discussion

Characterization of the photocatalysts

The characteristics of the prepared photocatalyst samples are summarized in Table 1. Figure 1 shows the SEM images of the prepared photocatalyst samples. The average particle sizes of the samples were estimated by measuring their apparent sizes, i.e., diameters of spherical particles or diagonal lengths of polyhedron particles, in the images. The particles size increased and then decreased with increasing amount of nitric acid. The XRD patterns for all the samples contained diffraction peaks that appeared at approximately 25.3°, 37.8°, 48.1°, 53.9°, and 54.8° as shown in Figure 2. These peaks coincided with the typical pattern of anatase-type TiO_2. The crystallite sizes were estimated from the strongest peaks at 25.3°. The order of samples with large crystallite size is different from that of samples with large particle size, as shown in Table 1. The particle size increased and then decreased with increasing amount of added nitric acid. On the other hand, the specific surface area decreased and then increased with increasing amount of added nitric acid. Crystallite size depends on rate of the phase transition of the systems during heating and on the acidity, i.e.,

on the structure of the precursors [24]. The particles consist not only of crystalline phases but also of amorphous phases with an agglomerating property [25]. The amorphous-rich particles are expected to have a large size because the amorphous phase agglomerates the crystalline particles. The specific surface areas of the samples are related to particle size. The amounts of TCE and DCAC adsorbed on the samples also depend on surface area. Increases and decreases of these characterized quantities occur with increasing amount of added nitric acid. Nitric acid acts as a catalyst for the hydrolysis and as an oxidizer, and accelerates the sol-gel reaction and crystallization. However, in some cases, nitric acid also prevents polymerization or crystallization, because it remains in the samples. Hydrochloric acid enhances the nucleation of TiO_2 compared with nitric acid [24]. Hydrochloric acid is easily evaporated after promoting the rearrangement of TiO_6 octahedra.

(Figures 1 and 2)

Figure 3 shows XPS spectra of the N 1s electron for the samples at approximately 400 eV. There was no peak in the spectrum of sample, N0, prepared without nitric acid. In the samples prepared with nitric acid, peaks were clearly observed at 398-399 eV. This band is assigned to the O-N bond in some nitrogen oxide species present in the system [5,7,21,26]. The result of the XPS analysis supports N-doping of the TiO_2 by use of our procedure even though there was not an obvious 396 eV band assigned to the Ti-N bond produced by

replacement of oxygen in the TiO_2 lattice with nitrogen [3−5,7,12,21]. The samples prepared with nitric acid are regarded as N-doped TiO_2 whereas the sample prepared without nitric acid is regarded as undoped TiO_2. The XPS peaks of Ti 2p and O 1s for all the samples were located at 458.6 and 529.8 eV, respectively, because the amounts of the nitrogen species were too low to affect their bands. The N/Ti atomic ratios for the samples were also estimated by XPS analysis, as shown in Table 1. The amount of doped nitrogen increased and then decreased with increasing amount of added nitric acid. The TiO_2 was not necessarily doped with more nitrogen as a result of adding more nitric acid to the system. This is expected to depend on the reaction in the systems during the sol-gel transition and on the crystallization process. The is discussed in more detail in the section “Mechanism of nitrogen doping”.

(Figure 3 and Table 1)

Figure 4 shows the UV-visible diffuse reflectance spectra of the prepared samples. The ordinate indicates the Kubelka-Munk function approximating the absorbance. The N-doped TiO_2 samples obviously absorb visible light from 400 to 450 nm, whereas the absorption edge of the undoped TiO_2 sample, N0, is located at approximately 400 nm. Therefore, the N-doped TiO_2 probably utilizes visible light more efficiently than the undoped TiO_2. This result indicates that the TiO_2 was definitely doped with nitrogen, and that an

impurity band was formed above the valence band of the TiO_2 because the shifts in the absorption edge for the samples correspond to the amount of the doped nitrogen, which was estimated by XPS analysis.

(Figure 4)

Figure 5 shows FTIR spectra obtained from samples before and after heating. The samples before heating are amorphous gels dried at room temperature. The spectrum of the dried gel of the undoped sample, N0, mainly contains bands originating from the OH-bending of adsorbed water (1630 cm^{-1}), tetrahedral TiO-stretching (840 cm^{-1}) [27], and octahedral TiO-stretching (560 cm^{-1}) [27–30]. In addition to these peaks, spectra of the N-doped samples contained a band for the NO-stretching of NO_3^- (1385 cm^{-1}). Furthermore, the following band intensities increased with increasing amount of nitric acid: the C=O-stretching (1720 cm^{-1}) and the CC-stretching or the CO-stretching and OH-bending (1400 cm^{-1}) for acetaldehyde or acetic acid, the NO-stretching (1690–1610 cm^{-1}) for ethyl nitrite, and the NO_2^--symmetric (1250 cm^{-1}) and anti-symmetric (800 cm^{-1}) stretching for NO_2^-. The band intensity of NO_3^- increased and decreased with increasing amount of nitric acid added to the system. Relatively greater intensity of the tetrahedral and octahedral TiO-stretching band was observed for the sample prepared using greater amounts of nitric acid. Nitric acid acts as not only a catalyst for hydrolysis of titanium alkoxide but also as an oxidizer. The

ratios of nitric acid to titanium in N02, N1, N5, and N10 are 0.14, 0.70, 3.5, and 7.0, respectively. As excess nitric acid over that required for hydrolysis of the TTIP reacted with the ethanol solvent and with the titanium species, it was reduced to NO_2^- or ethyl nitrite. Consequently, the growth of the titania networks was promoted by the nitric acid.

(Figure 5)

After the heat treatment, the intensities of bands from adsorbed water, the oxidation products of ethanol, and the nitrogen species drastically decreased. In addition to these, the relative intensity of the tetrahedral TiO band decreased and that of the octahedral TiO band increased. These results indicate that the TiOH groups are further polymerized and that the resulting water molecules were evaporated by heating. These results also indicate that absorption of visible light does not originate from Ti complexes with organic compounds, because organic compounds are hardly observed, even in FTIR spectra obtained from the dried gels before heating. Nitrogen species were barely observed by FTIR measurement after heating the samples, because the TiO_2 was doped with very small amounts only, as was confirmed by XPS analysis.

Mechanism of nitrogen doping

XPS analysis showed the TiO_2 was doped with nitrogen oxide species. The FTIR spectra of the samples during the sol-gel transition were also studied in order to clarify the

reaction of the nitrogen species and the nitrogen-doping mechanism. Figure 6 shows the changes in the FTIR spectra of sample N10 during the sol-gel transition with and without ultrasonic irradiation before gelation of the system. In the sol sample just after its preparation, the spectrum contained bands at 1380, 1350, 1090, 1050, and 880 cm^{-1} for the ethanol solvent. In addition, bands at 1660, 1290, and 950 cm^{-1} for ethyl nitrate were observed, because of the esterification reaction between ethanol and nitric acid. As the sol-gel reaction proceeded with ultrasonic irradiation, the bands for ethanol and ethyl nitrate decreased in intensity, and the bands at 1720 cm^{-1} for acetaldehyde or acetic acid, at 1690–1610 cm^{-1} for ethyl nitrite, at 1385 cm^{-1} for NO_3^-, and at 1250 cm^{-1} for NO_2^- increased in intensity. The tetrahedral and octahedral TiO-stretching bands at 840–560 cm^{-1} for the titania networks were also enhanced after six days. These results indicated that the ethanol and the titanium species were oxidized by nitric acid during the sol-gel transition. NO_3^- immediately reacted with ethanol and produced ethyl nitrate just after preparation of the sol. The NO_3^- was released from the ethyl nitrate during evaporation of the ethanol solvent and ionically bonded to the titanium species at approximately the gelation time. The spectral change was observed during ultrasonic irradiation; only a slight change was observed without ultrasonic irradiation for six days. The ultrasonic irradiation promoted the sol-gel reaction, especially evaporation of the ethanol solvent, oxidation by nitric acid, and polymerization of

the titanium species. The NO_2^- produced by reduction of NO_3^- also reacted with ethanol and produced ethyl nitrite in the sol system. The NO_2^- can also be ionically bonded to the titanium species, because of evaporation of ethanol at approximately the gelation time. However, the amount of this species is expected to be lower than that of the NO_3^- bonded to the titanium species, because NO_2^- is easily evaporated or decomposed. A greater amount of nitric acid caused an exothermic reaction and promoted oxidation of ethanol and the titanium species, thus consuming the nitric acid. Consequently, a greater amount of NO_3^- remained in N1 and N5 than in N10 after their gelation. These results agree with the amounts of the nitrogen species in the doped TiO_2 as shown in Table 1. The TiO_2 was doped with nitrogen oxide species, i.e., NO, as a result of reduction of the NO_3^- bonded to the titania networks. A greater amount of the NO was placed in the titania networks after heating of the gel samples in which a greater amount of NO_3^- was incorporated. The preparation process of the gel samples before heating is important for nitrogen doping. These results also indicated that reduction of NO_3^- to NO_2^- and further decomposition to NO occurred during not only the sol-gel transition but also during the heating process.

(Figure 6)

Although NO_3^- acts as a oxidizer, in some cases, it also prevents crystallization. Sample, N1, has the largest particle size, the smallest crystallite size, the greatest amount of

nitrogen species, and the lowest specific surface area of all the samples. The nitrogen species produced the residual amorphous phase consisting of large particles and defects in the crystalline particles and on their surface.

The relationship between the structure and the amount of the doped nitrogen is summarized below. The amorphous-rich, i.e., small crystallite-sized, particles were large, because the amorphous phase agglomerated the small crystalline particles. Samples consisting of larger particles had lower specific surface areas. The particle size of the N-doped TiO_2 increased and then decreased with increasing amount of added nitric acid. On the other hand, the specific surface area decreased and then increased with increasing amount of added nitric acid. In the system containing an amount of nitric acid smaller than a specific amount, the nitric acid remaining in the sample prevents polymerization and crystallization. A much greater amount of nitric acid caused an exothermic reaction and promoted the oxidation of the titanium species and supported their crystallization by consuming the nitric acid. These results indicate that the amount of nitric acid affected the particle size and crystallization of TiO_2. Consequently, the amount of the doping nitrogen increased and then decreased with increasing amount of added nitric acid.

Photocatalytic degradation of TCE

Photocatalytic degradation of TCE was investigated by use of the prepared samples and

irradiation with UV or visible light. Three typical characteristic IR bands of TCE at 944 cm^{-1} (C-Cl stretching), 849 cm^{-1} (C-Cl stretching), and 783 cm^{-1} (C-H bending) rapidly decreased during the UV irradiation. In addition to these, CO (2231–2066 cm^{-1}), CO_2 (2398–2280 cm^{-1}), $COCl_2$ (856 cm^{-1}), HCl (3037–2723 cm^{-1}), and DCAC (800 and 741 cm^{-1}) were mainly produced during the reaction [5,6,22,31−33]. The degradation of TCE was confirmed by these IR measurements, as reported in the literature [5,20,22,31.34−37]. During irradiation with visible light, TCE was degraded and CO, CO_2, HCl, and $COCl_2$ were generated, similarly to during UV irradiation. However, no DCAC was found in this case, similar to results reported elsewhere [5,20].

The time course of the relative amounts of TCE and each product were estimated by analyzing their FTIR spectra. Figure 7 shows the time course of the relative concentration of TCE estimated from the IR absorbance at 944 cm^{-1}. The average rates of degradation of TCE using the photocatalyst samples are shown in Table 2. TCE was degraded during 5–25-min UV irradiation using the prepared samples, indicating that all the prepared samples functioned as highly active photocatalysts. The order of the rate of degradation during UV irradiation was the same as that of the surface area of the photocatalysts. The activity of the photocatalyst samples strongly depended on their specific surface area rather than their crystallinity, because their crystallite sizes were not very different.

(Figure 7 and Table 2)

TCE was degraded during 90–150-min irradiation using samples, N1, N5, and N10, indicating visible light-induced activity. The rate of degradation was very slow using N02 even though it has the highest specific surface area and adsorption ability of all the samples. N0 had only a slight activity during visible light irradiation. Absorption of visible light by the samples depends on the amount of doped nitrogen, as shown in Figure 4 and Table 1. However, the order of the rate of degradation during irradiation with visible light was not the same as that of any characteristics of the photocatalysts. The rate of degradation depended on both their specific surface area and the visible absorption of the photocatalytic samples. High activity requires not only an increase in the amount of the doped nitrogen but also control of the nanostructure of the photocatalyst particles.

The degradation kinetics of TCE were affected by the complex reaction process of its intermediate products even though the average rates of degradation were estimated in order to compare the reactions using each photocatalyst shown in Table 2. The initial reaction is slightly affected by the consecutive reactions. The initial rates of degradation per unit surface area of the samples (250 mg) with strong absorption of visible light, i.e., N1, N5, and N10, were estimated to be 7.6, 4.7, and 4.3×10^{-7} mol dm^{-3} min^{-1} m^{-2}, respectively. These results indicate that the absorption of visible light induced by the N-doping is effective in the

degradation of TCE.

4. Conclusions

N-doped TiO_2 was prepared by use of sol-gel systems containing titanium alkoxide, and HNO_3 nitrogen source. The time needed for gelation of the system was drastically reduced by ultrasonic irradiation. The peaks assigned to NO_3^- and its reduced product, NO_2^-, and their compounds, were observed by FT-IR measurement during the sol-gel transition. The nitrogen oxide species were confirmed by observation of N-O peaks in the XPS spectrum of the sample heated at 400 °C. The NO_3^- species acted as oxidizers of the ethanol solvent and titanium species. The TiO_2 was doped with nitrogen oxide species as a result of reduction of the NO_3^- incorporated into the dried gel samples. A greater amount of NO species was present in the titania networks after heating of gel samples containing more NO_3^-. However, a large amount of nitric acid caused an exothermic reaction and promoted oxidation of ethanol and of the titanium species, which consumed the nitric acid. For systems containing more than a specific amount of nitric acid, the amount of doped nitrogen species decreased with increasing amount of added nitric acid, because its reduced product, NO_2^-, is easily evaporated or decomposed. The process of preparation of the gel samples before heating is important for nitrogen doping. The photocatalytic activity of the N-doped TiO_2

samples during irradiation with UV and visible light was confirmed by degradation of TCE. The activity of the photocatalyst samples during UV irradiation strongly depended on their specific surface areas rather than their crystallinities, because their crystallite sizes were not very different. The rate of degradation during visible irradiation depended on both the specific surface area and the visible absorption of the photocatalytic samples. The visible absorption induced by the N-doping was effective in the degradation of TCE.

Acknowledgment

The authors thank Professor Kenichi Tenya of this university for his technical assistance with XPS analysis.

References

[1] A. Fujishima, T. N. Rao, D A. Tryk, J. Photochem. Photobiol. C: Photochem. Rev. 1, 1 (2000)

[2] D. Chatterjee, S. Dasgupta, J. Photochem. Photobiol. C: Photochem. Rev. 6, 186, (2005)

[3] R. Asahi, T. Morikawa, T. Ohwaki, K. Aoki, Y. Taga, Science 293, 269 (2001)

[4] S. Yang, L. Gao, J. Am. Ceram. Soc. 87, 1803 (2004)

[5] S. K. Joung, T. Amemiya, M. Murabayashi, K. Itoh, Chem. Eur. J. 12, 5526 (2006)

[6] R. Nakamura, T. Tanaka, Y. Nakato, J. Phys. Chem. B 108, 10617 (2004)

[7] J. Wang, D. N. Tafen, J. P. Lewis, Z. Hong, A. Manivannan, M. Zhi, M. Li, N. Wu, J. Am. Chem. Soc. 131, 12290 (2009)

[8] C. W. H. Dunnill, Z. A. Aiken, J. Pratten, M. Wilson, D. J. Morgan, I. P. Parkin, J. Photochem. Photobiol. A: Chem. 207, 244 (2009)

[9] C. Sarantopoulos, A. N. Gleizes, F. Maury, Thin Solid Films 518, 1299 (2009)

[10] J. Wang, Z. Wang, H. Li, Y. Cui, Y. Du, J. Alloys Compd. 494, 372 (2010)

[11] L. Han, Y. Xin, H. Liu, X. Ma, G. Tang, J. Hazard. Mater. 175, 524 (2010)

[12] T. Ohsawa, M. A. Henderson, S. A. Chambers, J. Phys. Chem. C 114, 6595 (2010)

[13] S. Sato, Chem. Phys. Lett. 123, 126 (1986)

[14] T. Ihara, M. Miyoshi, Y. Iriyama, O. Matsumoto, S. Sugihara, Appl. Catal. B: Environ. 42, 403 (2003)

[15] D. P. Subagio, M. Srinivasan, M. Lim, T. Lim, Appl. Catal. B: Environ. 95, 414 (2010)

[16] A. R. Gandhe, S. P. Naik, J. B. Fernandes, Microporous Mesoporous Mater. 87, 103 (2005)

[17] H. Choi, M. G. Antoniou, M. Pelaez, A. A . De la Cruz, J. A. Shoemaker, D. D.

Dionysiou, Environ. Sci. Technol. 41, 7530 (2007)

[18] T. C. Jagadale, S. P. Takale, R. S. Sonawane, H. M. Joshi, S. I. Patil, B. B. Kale, S. B. Ogale, J. Phys. Chem. C 112, 14595 (2008)

[19] J. Ananpattarachai, P. Kajitvichyanukul, S. Seraphin, J. Hazard. Mater. 168, 253 (2009)

[20] Y. Yokosuka, K. Oki, H. Nishikiori, Y. Tatsumi, N. Tanaka, T. Fujii, Res. Chem. Intermed. 35, 43 (2009)

[21] C. X. Dong, A. P. Xian, E. H. Ham, J. K. Shang, J. Mater. Sci. 41, 6168 (2006)

[22] K. Oki, S. Tsuchida, H. Nishikiori, N. Tanaka, T. Fujii, Int. J. Photoenergy 5, 11 (2003)

[23] K. Oki, S. Yamada, S. Tsuchida, H. Nishikiori, N. Tanaka, T. Fujii, Res. Chem. Intermed. 29, 827 (2003)

[24] H. Yin, Y. Wada, T. Kitamura, S. Kambe, S. Murasawa, H. Mori, T. Sakata, S. Yanagida, J. Mater. Chem. 11, 1694 (2001)

[25] A. J. Maira, K. L. Yeung, C. Y. Lee, P. L. Yue, C. K. Chan, J. Catal. 192, 185 (2000)

[26] S. Sato, R. Nakamura, S. Abe, Appl. Catal. A: Gen. 284, 131 (2005)

[27] P. Tarte, Physics of Non-Crystalline Solids, (North Holland, Amsterdam, 1965), p. 549.

[28] M. L. Galzada, L. Delolmo, J. Non-Cryst. Solids 121, 413 (1990)

[29] S. Ben Amor, G. Baud, J. P. Besse, M. Jacquet, Mater. Sci. Eng. B 47, 110 (1997)

[30] L. Castañeda, J. C. Alonso, A. Ortiz, E. Andrade, J. M. Saniger, J. G. Bañuelos, Mater. Chem. Phys. 77, 938 (2002)

[31] P. B. Amama, K. Itoh, M. Murabayashi, J. Mol. Catal. A: Chem. 176, 165 (2001)

[32] J. S. Kim, K. Itoh, M. Murabayashi, B. A. Kim, Chemosphere 38, 2969 (1999)

[33] M. Kang, J. H. Lee, S. H. Lee, C. H.Chung, K. J. Yoon, K. Ogino, S. Miyata, S. J. Choung, J. Mol. Catal. A: Chem. 193, 273 (2003)

[34] W. A. Jacoby, M. R. Nimlos, D. M. Blake, R. D. Noble, C. A. Koval, Environ. Sci. Technol. 28, 1661 (1994)

[35] J. Fan, J. T. Yates, Jr., J. Am. Chem. Soc. 118, 4686 (1996)

[36] M. D. Driessen, A. L. Goodman, T. M. Miller, G. A. Zaharias, V. V. Grassian, J. Phys. Chem. B 102, 549 (1998)

[37] J. S. Kim, K. Itoh, M. Murabayashi, Chemosphere 36, 483 (1998)

Table 1 Characteristics of the prepared catalysts.

	N0	N02	N1	N5	N10
Particle size / nm	18 ± 6	20 ± 5	29 ± 8	26 ± 5	22 ± 7
Crystallite size / nm	8.6 ± 0.6	8.4 ± 0.2	7.9 ± 0.7	8.4 ± 0.8	8.8 ± 0.9
Specific surface area / m^2g^{-1}	88	97	22	56	73
TCE adsorption / mol g^{-1}	4.6×10^{-5}	8.5×10^{-5}	2.5×10^{-5}	4.2×10^{-5}	4.5×10^{-5}
DCAC adsorption / mol g^{-1}	2.4×10^{-3}	4.0×10^{-3}	1.5×10^{-3}	1.7×10^{-3}	3.0×10^{-3}
N/Ti ratio / %	0.00	0.01	0.48	0.37	0.17

Table 2 Average rates of degradation of TCE (mol dm^{-3} min^{-1}) using the prepared catalysts.

	N0	N02	N1	N5	N10
UV irradiation	5.5×10^{-5}	6.9×10^{-5}	1.3×10^{-5}	2.0×10^{-5}	2.4×10^{-5}
visible irradiation	-	9.6×10^{-8}	2.3×10^{-6}	2.7×10^{-6}	4.5×10^{-6}

Figure captions

Figure 1 SEM images of (a) N0, (b) N02, (c) N1, (d) N5, and (e) N10

Figure 2 XRD patterns of (1) N0, (2) N02, (3) N1, (4) N5, and (5) N10

Figure 3 N 1s XPS spectra of (1) N0, (2) N02, (3) N1, (4) N5, and (5) N10

Figure 4 UV-visible diffuse reflectance spectra of (1) N0, (2) N02, (3) N1, (4) N5, and (5) N10 expressed using the Kubelka-Munk function approximating the absorbance

Figure 5 FTIR spectra of (1) N0, (2) N02, (3) N1, (4) N5, and (5) N10 observed (a) before and (b) after heating at 400°C

Figure 6 Changes in the FTIR spectra of the sol containing 10.0 cm^3 of nitric acid, which is the precursor of N10, during the sol-gel reaction (a) with and (b) without ultrasonic irradiation : (1) just after the preparation, (2) after 3 days, (3) after 6 days

Figure 7 Time course of the relative concentration of TCE during photocatalytic degradation of TCE using (1) N0, (2) N02, (3) N1, (4) N5, and (5) N10 during (a) UV or (b) visible irradiation

Figure 1

(a)

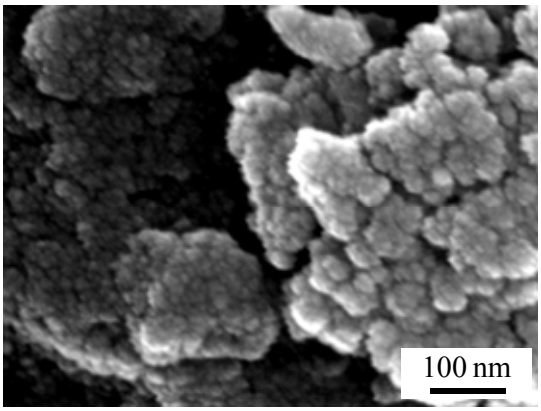

(b)

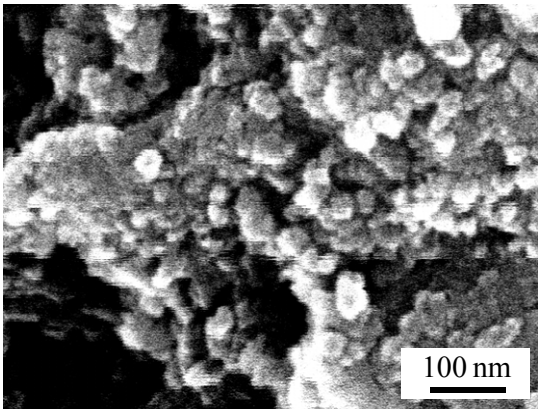

(c)

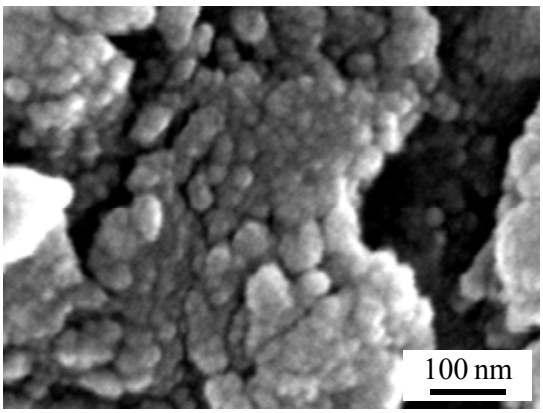

(d)

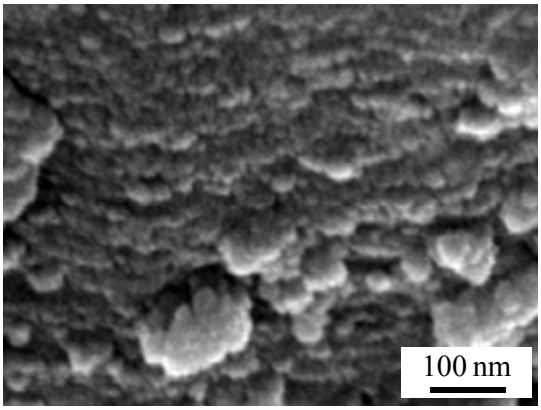

(e)

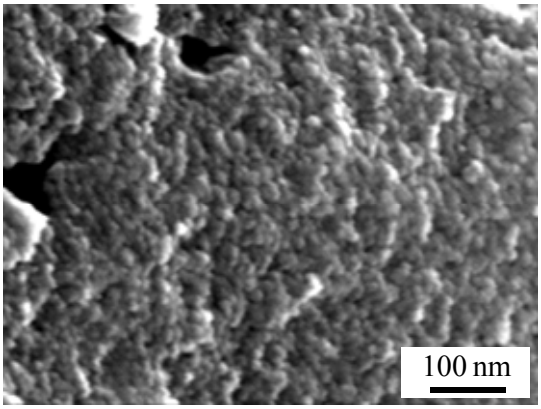

Figure 2

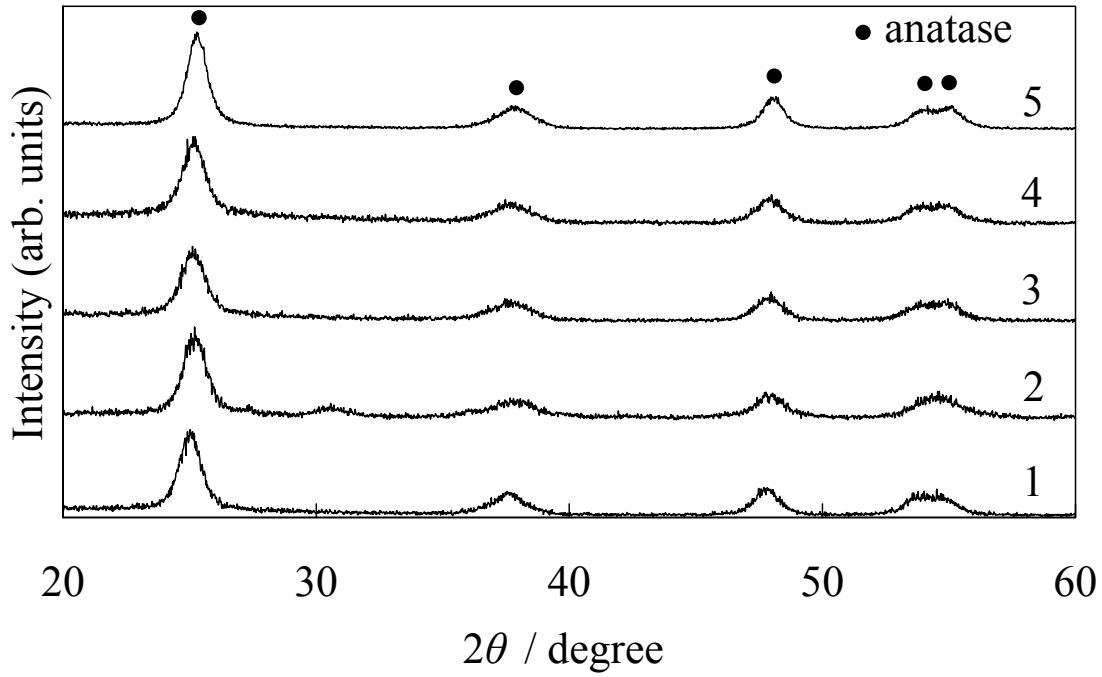

Figure 3

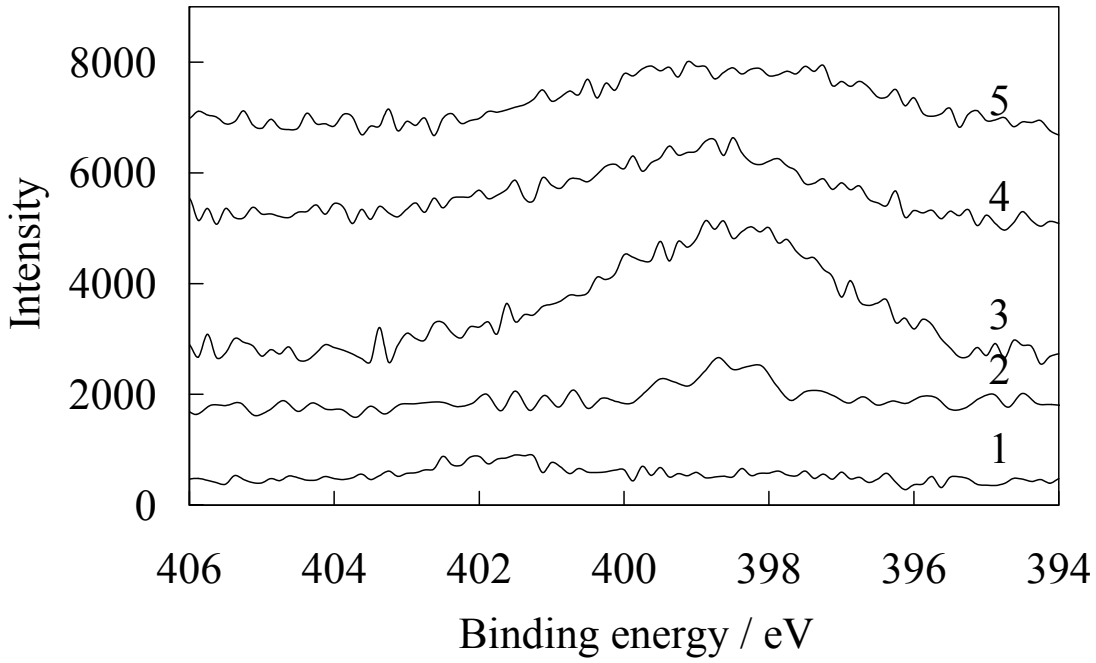
8000
6000
4000
2000
0
Intensity
5
4
3
2
1
406
404
402
400
398
396
394
Binding energy / eV

Figure 4

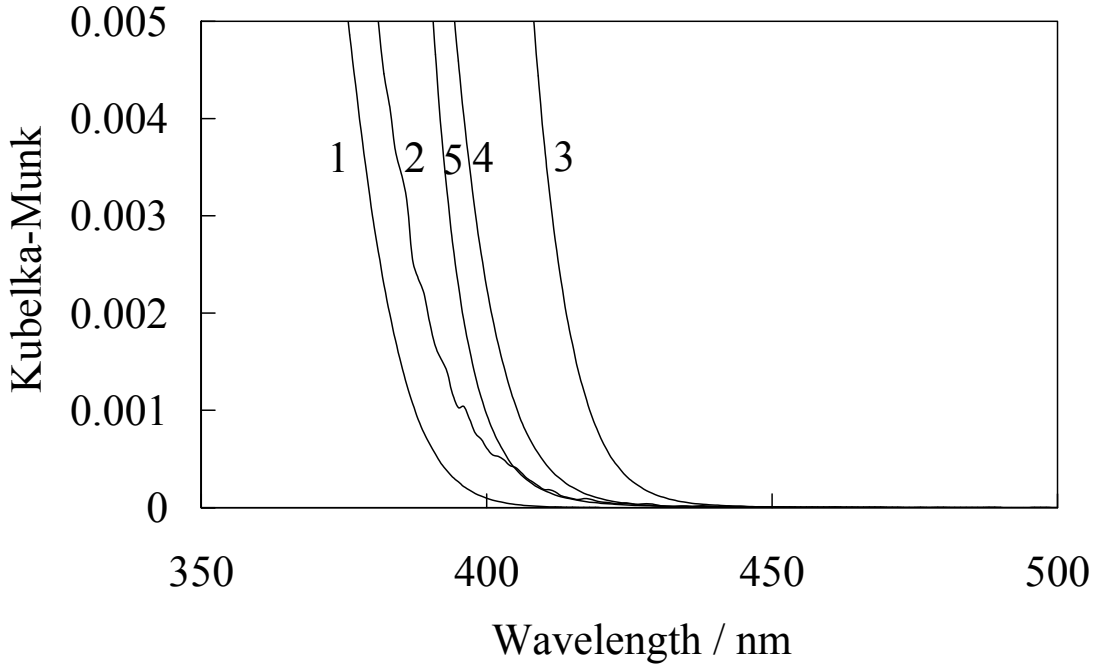
0.005
0.004
0.003
0.002
0.001
0
Kubelka-Munk
1
2
5
4
3
350
400
450
500
Wavelength / nm

Figure 5

(a)

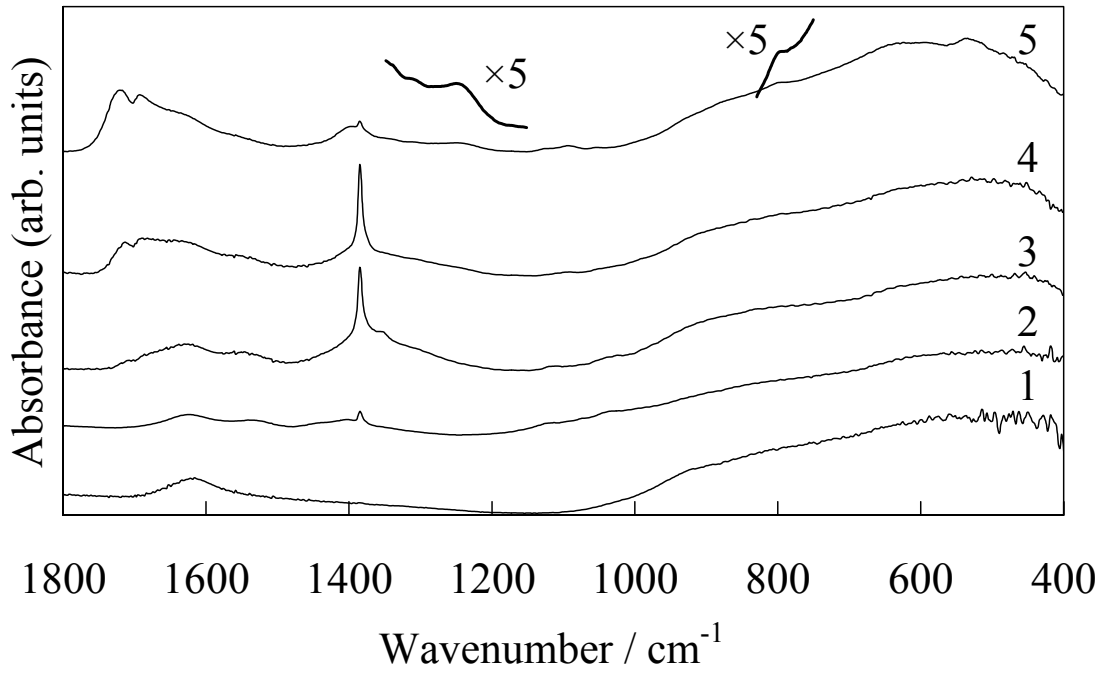
Absorbance (arb. units)
×5
×5
5
4
3
2
1
1800
1600
1400
1200
1000
800
600
400
Wavenumber / cm-1

(b)

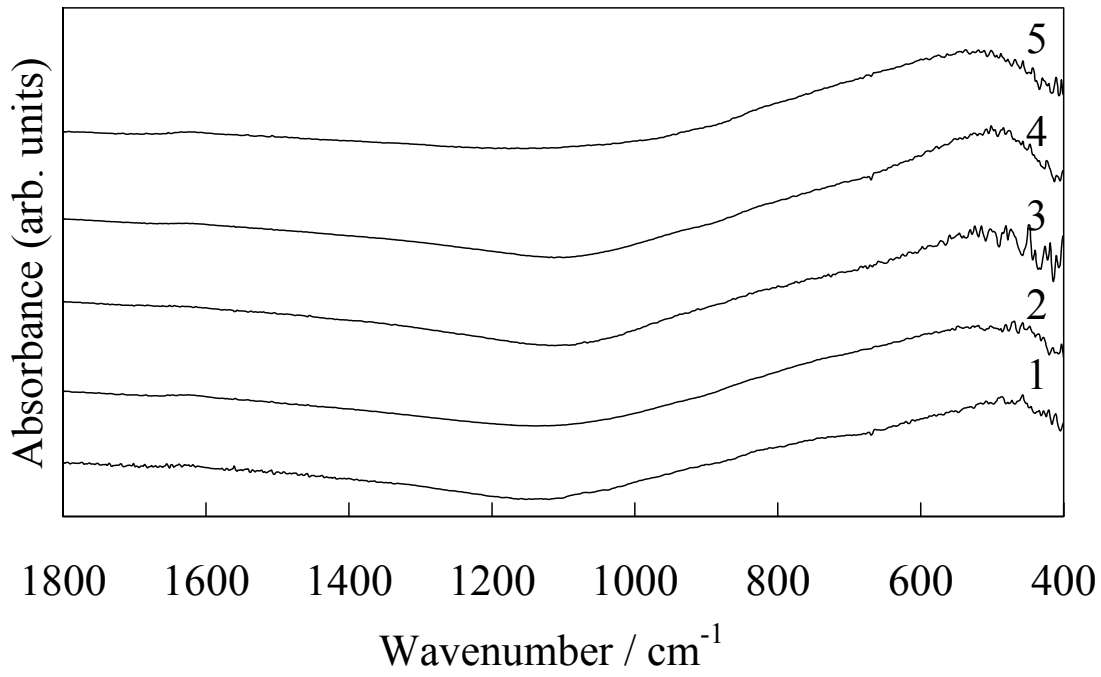
Absorbance (arb. units)
5
4
3
2
1
1800
1600
1400
1200
1000
800
600
400
Wavenumber / cm-1

Figure 6

(a)

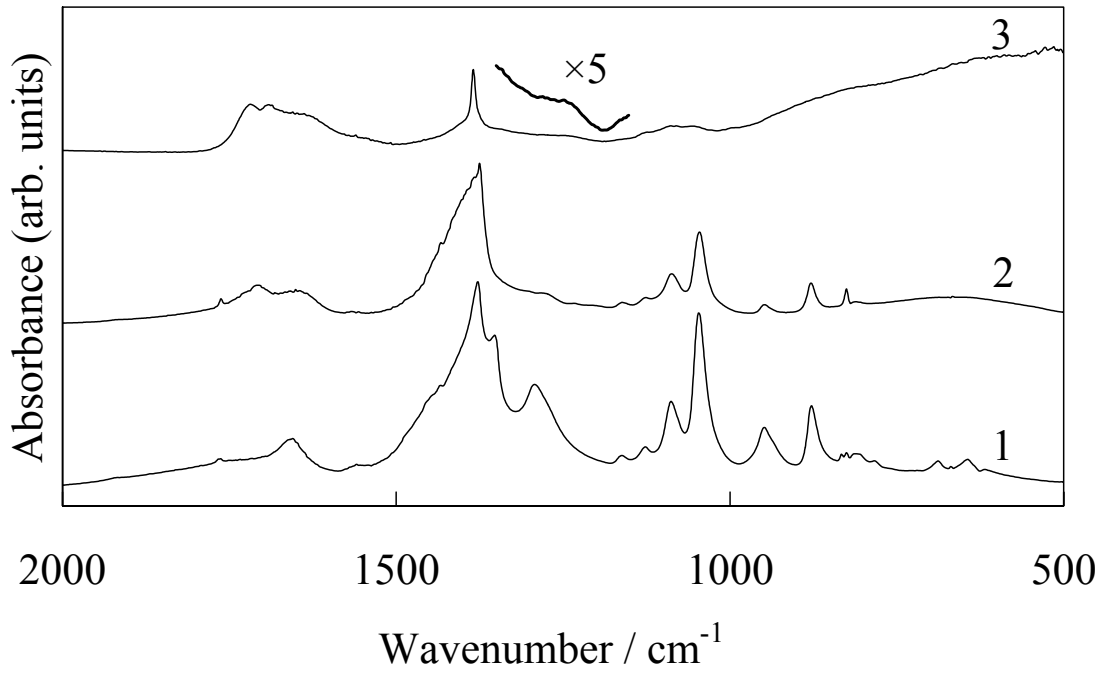
Absorbance (arb. units)
×5
3
2
1
2000
1500
1000
500
Wavenumber / cm-1

(b)

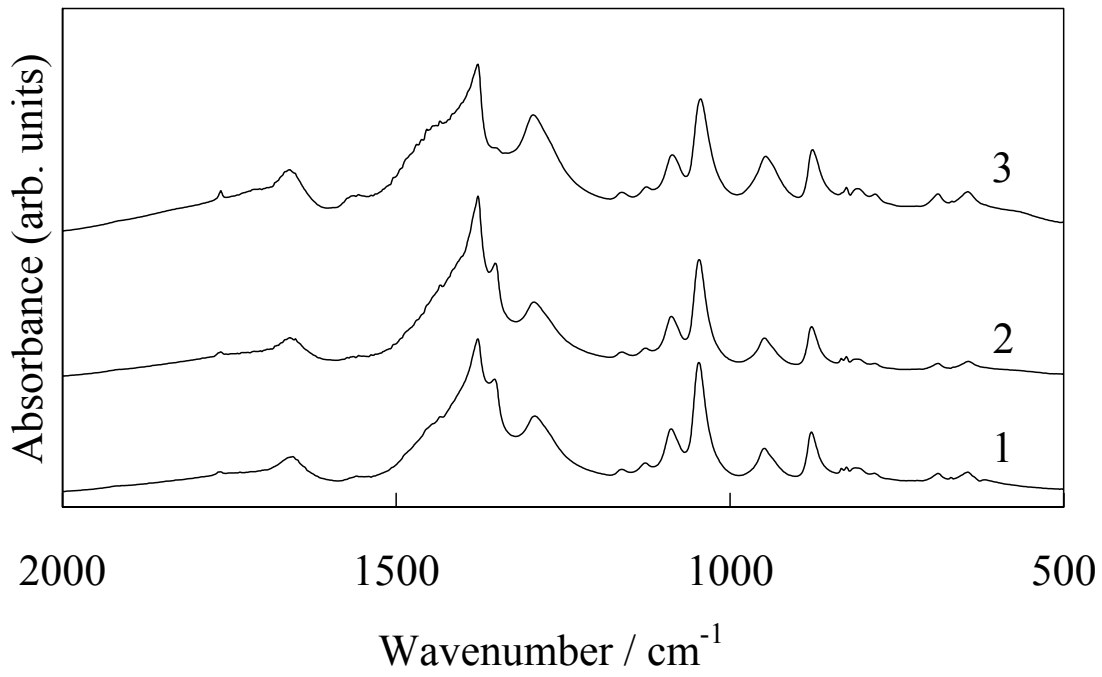
Absorbance (arb. units)
3
2
1
2000
1500
1000
500
Wavenumber / cm-1

Figure 7

(a)

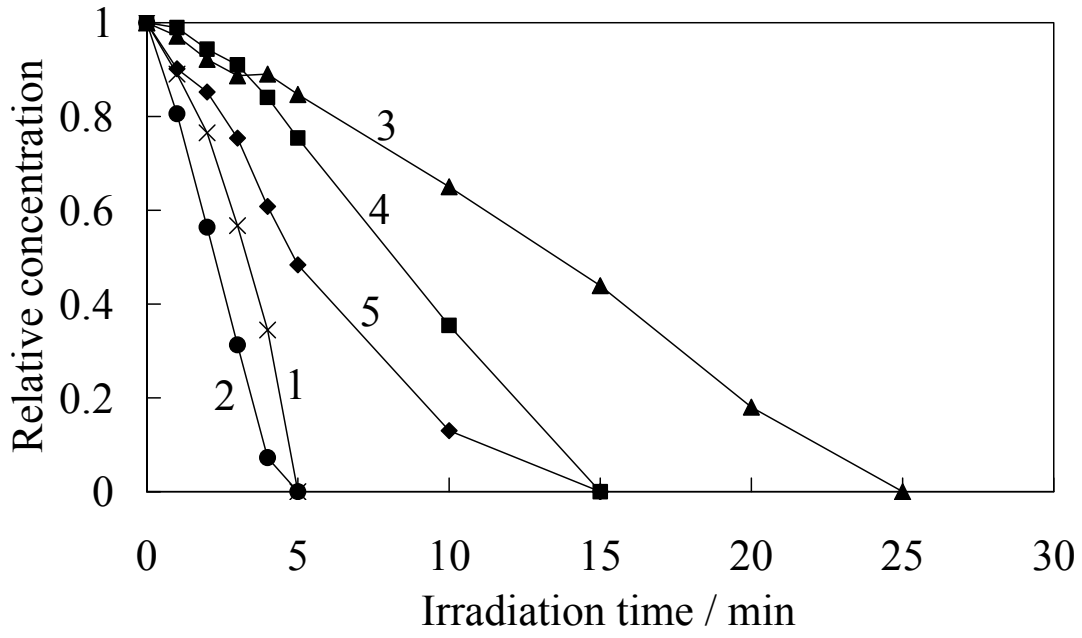
Relative concentration
1
0.8
0.6
0.4
0.2
0
0
5
10
15
20
25
30
Irradiation time / min
1
2
3
4
5

(b)

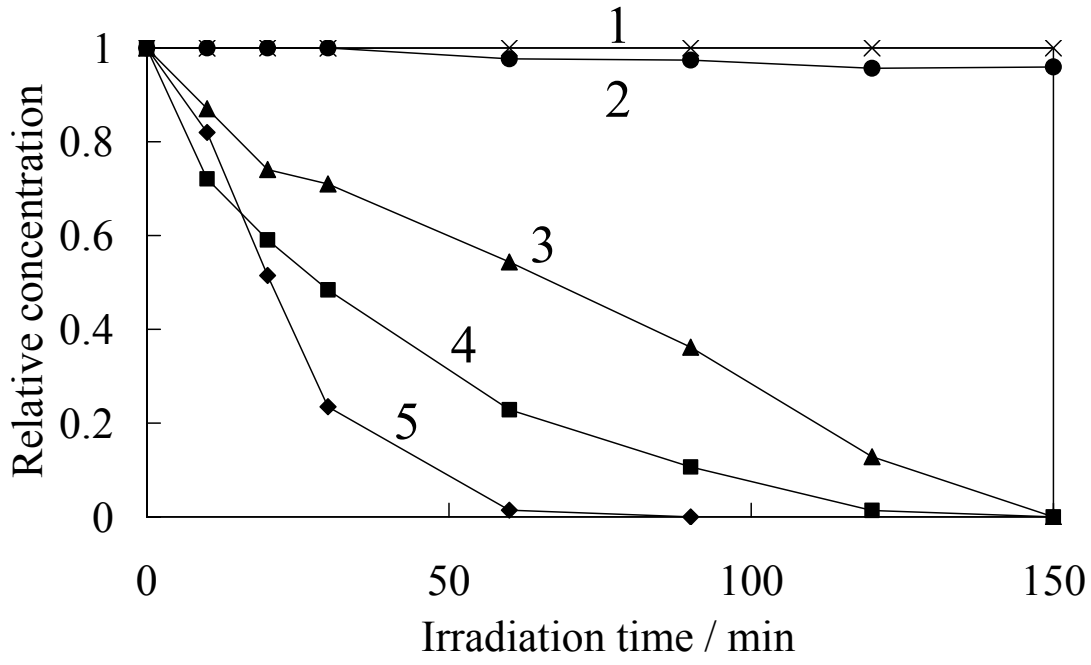
Relative concentration
1
0.8
0.6
0.4
0.2
0
0
50
100
150
Irradiation time / min
1
2
3
4
5